Journal of Nondestructive Evaluation (2024) 43:37
https://doi.org/10.1007/s10921-024-01055-y

Reconstruction of the Ferromagnetic Hysteresis in the Rayleigh Regime by Means of Impedance Analysis of the Excitation Coil

Sascha Thieltges[1] · Sargon Youssef[2] · Uwe Hartmann[3]

Received: 12 December 2023 / Accepted: 16 February 2024

Abstract
Ferromagnetic hysteresis measurements can be used to determine both magnetic and mechanical state variables that correlate with each other. Therefore, hysteresis measurements are suitable for mechanical material characterization. The application of standardized hysteresis measurement methods is complex and can only be used to a limited extent in an industrial environment. In this work, a BH (ferromagnetic hysteresis) curve is to be reconstructed on 22NiMoCr3-7 samples that are in different mechanically deformed states (different histories). The reconstruction of the hysteresis is performed by an impedance analysis of the H-field generating coil. The applied method demonstrates that the ferromagnetic hysteresis can be reconstructed by means of an impedance analysis and is sensitive to different states of plastical deformation.

Keywords Ferromagnetic hysteresis · Yoke · Rayleigh regime · Impedance analysis

1 Introduction

Due to the bidirectional coupling between magnetic parameters and the mechanical stress state (magnetoelasticity) of ferromagnetic materials, magnetic testing methods are suitable for characterizing mechanical stress [1–3]. These methods include: Magneto-optical methods [4, 5], Barkhausen noise analysis [6–8], magnetic flux leakage methods [8, 9] and standardized hysteresis measurement methods [10]. The signals from the various methods offer insights into the sample material at varying depths and across diverse time frames. For example, mechanical stresses can be measured by magneto-optical methods at the sample surface, by Barkhausen noise from zero to ≈200 μm depth [11] and by hysteresis measurement methods from zero to the entire sample cross-section. Standardized hysteresis measurement methods [10] exist, which are not easy to implement in industrial applications, as often the sample to be examined must be geometrically adapted (via a non-destructive way) and a sample-encompassing magnetizing and receiving coil have to be used. An alternative to standardized hysteresis measurement methods is the use of a yoke in an attachment technique [12–16]. In this setup, a coil (magnetizing coil) is wound around a soft magnetic yoke and the yoke is used to direct the H-field into the sample. By applying a periodic signal to the magnetizing coil, both the hysteresis of the magnetizing coil with the yoke and that of the sample are passed through simultaneously. The magnetic response function of the sample can be measured using various techniques:

1. With a further coil (pick-up-coil, PUC) wound around the yoke, which measures the magnetic flux in the magnetic circuit [14–19].
2. With a hall probe positioned between the legs of the yoke, measuring the magnetic field strength close to the sample surface [20, 21].

Another possibility is the analysis of voltage and current at the magnetization coil. In the work of Artetxe et al. [14–16] a current imprint is used and the voltage drop across

✉ Sascha Thieltges
sascha.thieltges@izfp.fraunhofer.de

Sargon Youssef
sargon.youssef@izfp.fraunhofer.de

Uwe Hartmann
u.hartmann@mx.uni-saarland.de

[1] Sensorphysics, Fraunhofer Institute for Nondestructive Testing IZFP, Campus E3 1, Saarbrücken 66123, Saarland, Germany

[2] Material Characterization, Fraunhofer Institute for Nondestructive Testing IZFP, Campus E3 1, Saarbrücken 66123, Saarland, Germany

[3] Institute of Experimental Physics, Saarland University, Campus C6 3, Saarbrücken 66123, Saarland, Germany

Published online: 16 March 2024

the magnetization coil is measured and analysed. In combination with a Hall probe, which measures the H field near the sample surface, the equivalent hysteresis (yoke + sample) is determined. The equivalent hysteresis is controlled to saturation. In the work of Moorthy [22–25], the voltage drop across the magnetisation coil is also analysed without explicitly determining hysteresis curves. Moorthy instead uses a voltage imprint. Another possibility which is considered in this work, is an impedance analysis of the excitation coil, since the inductance of the magnetizing coil depends on the magnetic properties of the entire circuit [26]. This approach has the advantage of eliminating the need for additional coils or sensors with the limitations that the developed methodic is only applabale in low field excitations of the ferromagnetic hysteresis.

For sufficiently low excitation, the response can be described analytically through the Rayleigh model [27, 28]. Here, the occurring parameters are material and condition-dependent and can be expressed by the complex permeability, which in turn can be determined by an impedance analysis.

The aim of this work is to reconstruct the ferromagnetic hysteresis from an impedance analysis of the magnetizing coil over a wide frequency range and to compare it with the measured hysteresis. By varying the frequency, the depth range to be investigated is varied. The measurements are carried out with a soft magnetic yoke in the attachment technique on the material 22NiMoCr3-7, which is used in nuclear power plants (NPP) worldwide. The samples were employed in different plastically deformed states.

2 Rayleigh Hysteresis and Complex Permeability

Assuming small excitation the B-H relation can be described analytically by a quadratic approach, the so-called Rayleigh model [26–29]. The occurring parameters μ_A and ν in Eqs. (1) and (2) of the Rayleigh model are materials- and material-states-dependent:

$$B = (\mu_A + \nu H_0) + \frac{\nu}{2}(H^2 - H_0^2) \tag{1}$$

and

$$B = (\mu_A + \nu H_0) - \frac{\nu}{2}(H^2 - H_0^2). \tag{2}$$

μ_A describes the initial permeability, assuming a demagnetized state and if μ_A ist plotted against H for low H-values there will be a linear dependency between μ_A and H. The slope of the linear dependency is given by the parameter ν. The time-varying external magnetic field is described by H, where H_0 corresponds to the amplitude of H. Ascending and descending hysteresis branches are given by Eq. (1) and (2) respectively. The external magnetic field is generated by a coil, the so-called magnetizing coil. On the other hand, Eq. (3) shows the definition of the complex permeability. The real part of the complex permeability depends on the inductance L, see Eq. (4), and the imaginary part on the electrical resistance R, see Eq. (5), of the magnetizing coil.

$$\boldsymbol{\mu} = \mu_L - i\mu_R, \tag{3}$$

$$\mu_L = \frac{Ll}{N^2 A \mu_0} \tag{4}$$

and

$$\mu_R = \frac{Rl}{\omega N^2 A \mu_0}. \tag{5}$$

Other factors appearing in Eq. (4 and 5) such as l, N, A, ω stand for magnetic path length, number of turns of the magnetizing coil, cross-sectional area of the magnetizing coil and angular frequency of excitation. As shown in the work by Kneller [26], the Rayleigh parameters can be expressed by the complex permeability:

$$\mu_L = \mu_A + \nu H_0 \tag{6}$$

and

$$\mu_R = \frac{4}{3\pi}\nu H_0. \tag{7}$$

The equations (4) and (5) as well as (6) and (7) can be connected by inserting the expressions. In his work the inductivity L (real part of complex permeability) and resistance R (imaginary part of complex permeability) can be calculated from an impedance analysis.

The impedance analysis determines the phase shift between current and voltage and the complex value of the impedance. The connection between the Rayleigh model and the complex permeability can be made by assuming that the H-field is proportional to the current in the magnetizing coil:

$$H = \alpha I. \tag{8}$$

Using Eqs. (4)–(8), the analytical expression for the hysteresis (Eq. (1) and (2)) can be rewritten as:

$$\frac{B}{\alpha} = \pm\frac{3\pi}{8}\frac{\mu_R}{I_0}I^2 + \mu_L I \mp \frac{3\pi}{8}\mu_R I_0. \tag{9}$$

In summary, the measurement procedure can be described as follows: by measuring the current and voltage drop across the magnetizing coil and the resulting phase shift and impedance magnitude, L and R can be determined from Eqs. (4) and (5). Finally the ferromagnetic hysteresis is determined by Eq. (9).

3 Experiments

3.1 Materials and Methods

The chosen material 22NiMoCr3-7 originates from a cooling line of the NPP Kärlich (Germany) and had already been mechanically characterized in a previous study [30]. Starting point of the present work are cylindrical samples of the material 22NiMoCr3-7, which were stress-relieved and plastically deformed. The samples were plastically deformed to $\epsilon_1 = 0.82\%$ (Lüders range), $\epsilon_2 = 2\%$ and $\epsilon_3 = 4\%$ (uniform strain) of total strain respectively. Moreover, the reference sample is at $\epsilon_0 = 0\%$ of total strain. For the present work, the magnetic measurements were carried out with a FeSi yoke in an attachment technique in the middle region of the cylindrical specimens. The yoke is composed of individual sheets to suppress eddy currents and was adapted to the specimen geometry to reduce stray magnetic fields. Figure 1 shows the sensor application schematically. The magnetizing coil consists of 200 turns and the cross section is $1cm^2$ and the magnetic path length l is $8cm$. To verify the calculated hysteresis by the Rayleigh model, a pick-up coil was also used to determine the magnetic flux density B. Using a function generator (Agilent 33210A), a sinusoidal voltage is amplified by a bipolar operational amplifier (KEPCO BOP 72-6 M) and applied to the magnetizing coil. The current through the magnetizing coil was measured via a current clamp (Tektronix TCP2020). On the other side, the resulting voltage drop at the magnetizing coil and the voltage drop across the PUC were measured with an oscilloscope (LeCroy DSO 6104). All data were recorded by the oscilloscope and subsequently analyzed using Matlab.

At the beginning of each measurement, a demagnetization was performed by decreasing the amplitude of the applied magnetizing voltage linearly with time until it was zero. Starting from the demagnetized state, a fixed voltage magnetization amplitude was selected and the magnetizing frequency was varied from $f_{exc} = 0.1$ Hz to $f_{exc} = 100$ Hz. Initial amplitudes for current and voltage of the imprinted signal in the magnetizing coil at f_{exc} were $I_{max,peak} = 0.1211A$ and $U_{max,peak} = 0.3462V$. At each frequency, 100 cycles were recorded and averaged to improve the S/N ratio.

3.2 Determination of Phase and Impedance

Since AC coupling was set on the oscilloscope, DC offset compensation was performed first. Secondly, the data were Hilbert-transformed and the phase and magnitude of the impedance were determined. Since these are available throughout the time domain (one period), the data were averaged over one period and the corresponding standard deviation was determined. In Figs. 2 and 3 the magnitude and phase of the impedance are plotted versus the magnetization frequencies. For all sample conditions, the qualitative picture is the same: with increasing frequency, the impedance as well as the relative phase relationship between manganization current and voltage increases. Quantitatively, the values differ within the measured frequency range, the standard deviation is largest for all samples at around 30 Hz. An examination of the raw signals shows that harmonics occur which are not present at low and high frequencies. The relative phase shift shows that there is a common intersection at about 30 Hz. With respect to the impedance magnitude, the curves for stress state $\epsilon_2 = 2\%$ and $\epsilon_3 = 4\%$ lie on top of each other respectively.

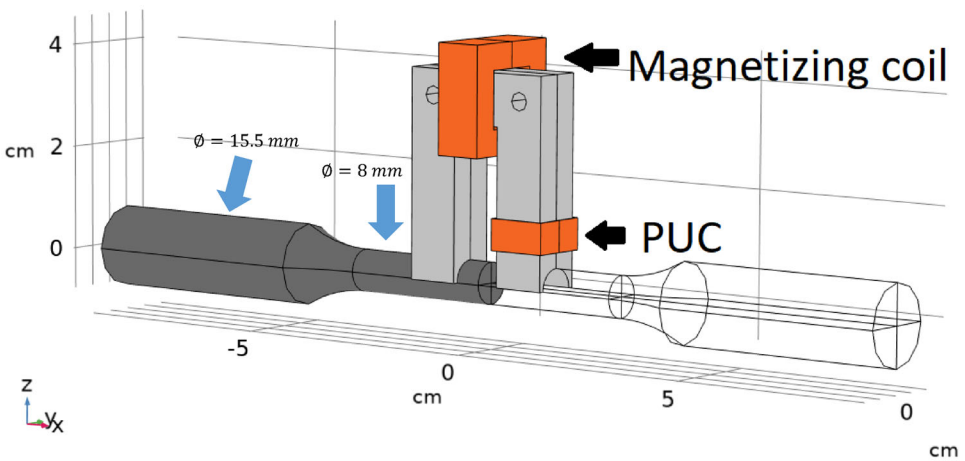

Fig. 1 Schematic representation of the sensor application on the cylindrical specimens. The sensor is adapted to the specimen geometry and is placed in the middle area of the specimen

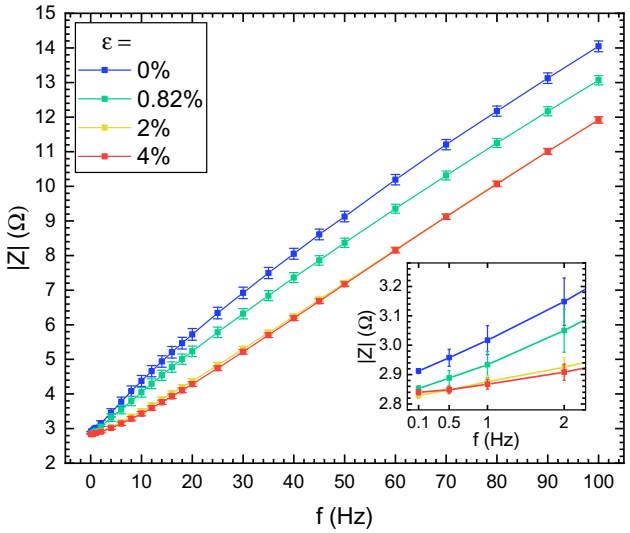

Fig. 2 Magnitude of impedance

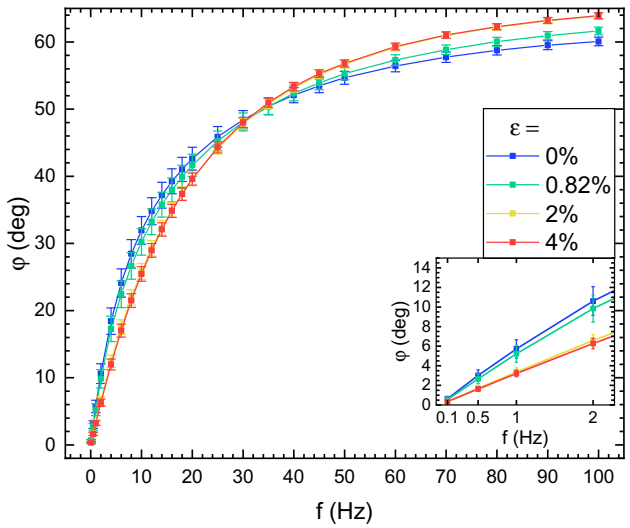

Fig. 3 Relative phase between magnetizing voltage and current

3.3 Determination of the Complex Permeability

The complex permeability was calulated by using Eq. (3), as shown in Figs. 4 and 5. The high error values result from the fact that the standard deviation was calculated according to the Gaussian error propagation and the error is proportional to the inverse of the frequency. I.e. small frequencies automatically produce a high error. Towards higher frequencies, the individual materials states asymptotically approach a parallel to the horizontal axis.

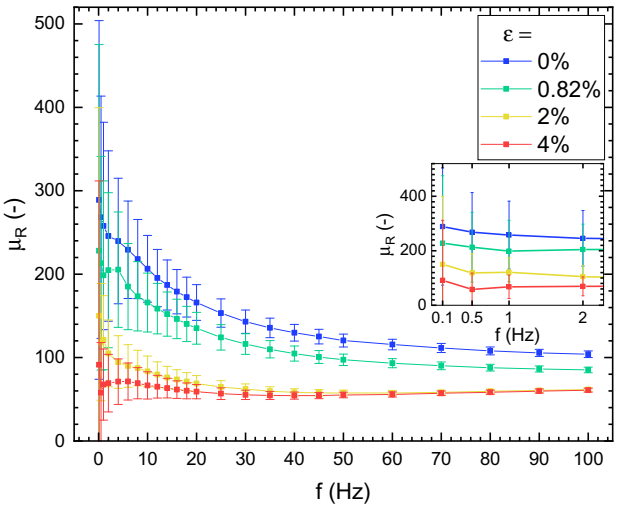

Fig. 4 Imaginary part of complex permeability

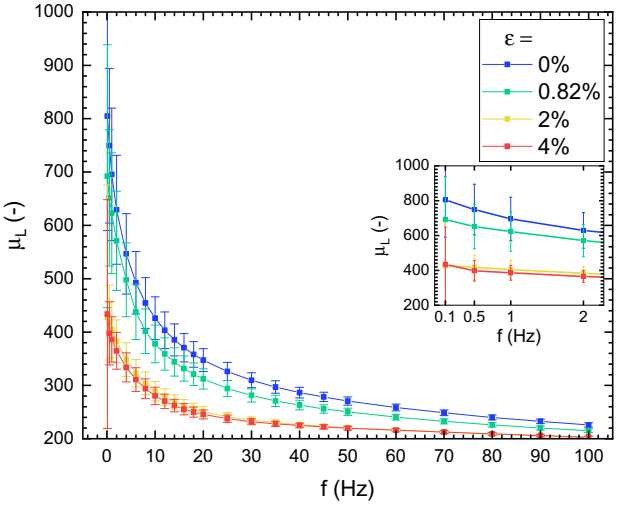

Fig. 5 Real part of complex permeability

3.4 Reconstruction of the Rayleigh Hysteresis

Based on the determined complex permeability, the hysteresis can be determined according to Eq. (9) up to a scaling factor α. In order to validate the calculated Rayleigh hysteresis curve, the magnetic flux density in the circuit was also measured by means of a PUC. By normalizing the data on the abscissa for each frequency, it is possible to compare the calculated hysteresis curves with the measured hysteresis ones. Figure 6 shows both the normalized calculated and the normalized measured hysteresis curves. The material state is $\epsilon_1 = 0.82\%$ and the magnetizing frequency 2 Hz. The shown data are normalized. To quantify how well calculated and measured hysteresis curves agree, the sum of the squared deviations was calculated (Fig. 7). Here it can be seen that remarkable accordance for all material states was achieved.

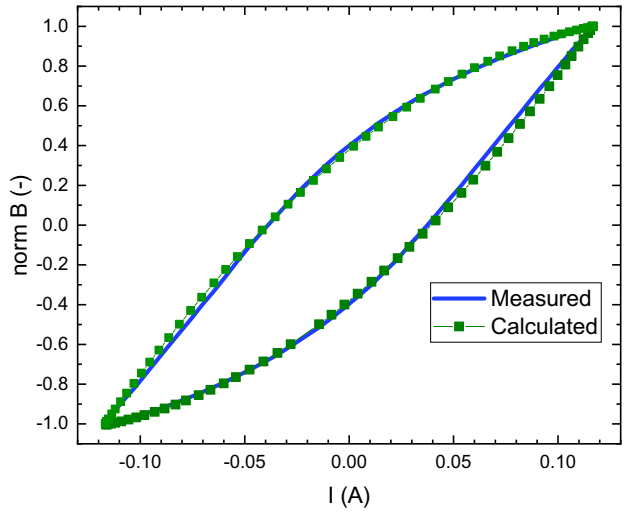

Fig. 6 Normalized measured and calculated hysteresis curve for the material state $\epsilon_1 = 0.82\%$ at $f_{exc} = 2Hz$

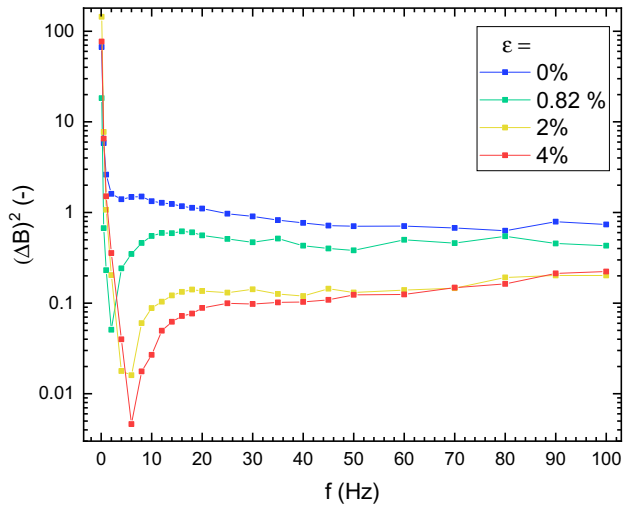

Fig. 7 Sum of the distance squares between measured and calculated hysteresis for the material states plotted against the magnetization frequency

For the $\epsilon_3 = 4\%$ mechanical load, the deviations are a minimum. For all four cases, it can be seen that the deviation is greatest at low frequencies.

3.5 Discussion

Compared to standard measurement methods for ferromagnetic hysteresis (for example Epstein-frame), the approach taken here, the use of a soft magnetic yoke in the attachment method, offers several advantages. In an industrial environment, it allows samples to be measured quickly. In addition, the sample does not have to be adapted to the sensor, but the sensor can be adapted to the sample. This possibility was exploited in the experiments performed. By using a soft magnetic yoke on a hard magnetic sample material, the magnetic resistance in the yoke becomes relatively small, making the sensor sensitive to changes in the magnetic circuit. However, as the samples were plastically deformed, the mechanical treatment results in microstructural changes such as a change in dislocation density or electrical conductivity, which are varyingly pronounced depending on the plastic deformation. As the mechanical properties change, the magnetization dynamics also change, resulting in a changed magnetic flux in the magnetic circuit.

The second approach pursued, the reconstruction of the superimposed hysteresis (yoke and sample) by applying the Rayleigh model is possible in the small field limit. Since the Rayleigh model is independent of the excitation frequency, it can be applied to a wide range of frequencies. This makes the Rayleigh parameters frequency-dependent. Another prerequisite that allows the Rayleigh model and impedance analysis to be used to reconstruct ferromagnetic hysteresis curves is the proportionality between the H-field and current in the magnetizing coil. This in turn is justified by considering Maxwell's equations.

Since both the yoke and the samples are magnetically different (soft and hard magnetic), the measured and reconstructed ferromagnetic hysteresis curves are a superposition of both curves respectively. In an industrial environment, however, this has the advantage that relative changes caused by changes in the sample material can be detected by using the same sensor in all measurements.

4 Conclusion

It has been shown that the superimposed ferromagnetic hysteresis can be reconstructed by an impedance analysis of the magnetizing coil using a yoke in the attachment method. The ferromagnetic hysteresis is superimposed as the ferromagnetic hysteresis of the yoke is soft and of the material hard. As the hysteresis itself is excited in a low H-field region the measured and calculated hysteresis curves are a effective hysteresis curve which depend on the hysteresis of the yoke and the material. Since the Rayleigh model for reconstructing ferromagnetic hysteresis is frequency-independent, it can be applied over a wide frequency range. The normalized hysteresis curves calculated by impedance analysis were compared with the normalized measured hysteresis curves. A comparison of the hysteresis curves shows good agreement.

Author Contributions All authors contributed to the study conception and design. Material preparation, data collection and analysis were performed by Sascha Thieltges. The first draft of the manuscript was written by Sascha Thieltges and Uwe Hartmann and all authors commented on previous versions of the manuscript. All authors read and approved the final manuscript.

Funding Open Access funding enabled and organized by Projekt DEAL.

Data availability No datasets were generated or analysed during the current study.

Declarations

Competing interests The authors declare no competing interests.

References

1. Altpeter, I., Theiner, W.A.: Eigenspannungsmessung an Stahl der Güte 22NiMoCr3 7 mit magnetischen und magnetoelastischen Prüfverfahren. 4. Internationale Konferenz Zerstörungsfreie Prüfung in der Kerntechnik (1981)
2. Jiles, D.C., Utrata, D.: Strain Dependence of the Magnetic Properties of AISI 4130 and 4140 Alloy Steels. In: Thompson, D.O., Chimenti, D.E. (eds). Review of Progress in Quantitative Nondestructive Evaluation, 1455–1462 (1988)
3. Sablik, M.J., Kwun, H., Burkhardt, G.L., Jiles, D.C.: Model for the effect of tensile and compressive stress on ferromagnetic hysteresis. J. Appl. Phys. **61**(8), 3799–3801 (1987). https://doi.org/10.1063/1.338650
4. Schroeder, G., Schäfer, R., Kronmüller, H.: Magneto-optical investigation of the domain structure of amorphous Fe80B20 alloys. Phys. Status Solidi **50**(2), 475–481 (1978). https://doi.org/10.1002/pssa.2210500215
5. Sander, D., Skomski, R., Enders, A., Schmidthals, C., Reuter, D., Kirschner, J.: The correlation between mechanical stress and magnetic properties of ultrathin films. J. Phys. Appl. Phys. **31**(6), 663–670 (1998). https://doi.org/10.1088/0022-3727/31/6/014
6. Capó Sánchez, J., Campos, M.F., Padovese, L.R.: Comparison Between Different Experimental Set-Ups for Measuring the Magnetic Barkhausen Noise in a Deformed 1050 Steel. J. Nondestruct. Eval. **36**(4), (2017) https://doi.org/10.1007/s10921-017-0445-1
7. Gupta, B., Uchimoto, T., Ducharne, B., Sebald, G., Miyazaki, T., Takagi, T.: Magnetic incremental permeability non-destructive evaluation of 12 Cr-Mo-W-V steel creep test samples with varied ageing levels and thermal treatments. NDT & E Int. **104**, 42–50 (2019). https://doi.org/10.1016/j.ndteint.2019.03.006
8. Wang, Z.D., Gu, Y., Wang, Y.S.: A review of three magnetic NDT technologies. J. Magnet. Magnet. Mater. **324**(4), 382–388 (2012). https://doi.org/10.1016/j.jmmm.2011.08.048
9. Xiao-meng, L., Hong-sheng, D., Shi-wu, B.: Research on the stress-magnetism effect of ferromagnetic materials based on three-dimensional magnetic flux leakage testing. NDT & E Int. **62**, 50–54 (2014). https://doi.org/10.1016/j.ndteint.2013.11.002
10. Bramerdorfer, G., Kitzberger, M., Wöckinger, D., Koprivica, B., Zurek, S.: State-of-the-art and future trends in soft magnetic materials characterization with focus on electric machine design – Part 1. tm - Technisches Messen 86(10), 540–552 (2019) https://doi.org/10.1515/teme-2019-0065
11. Stupakov, A., Perevertov, A., Neslušan, M.: Reading depth of the magnetic Barkhausen noise. I. One-phase semi-hard ribbons. J. Magnet. Magnet. Mater. 513, 167086 (2020) https://doi.org/10.1016/j.jmmm.2020.167086
12. Gabi, Y., Jacob, K., Wolter, B., Conrad, C., Strass, B., Grimm, J.: Analysis of incremental and differential permeability in NDT via 3D-simulation and experiment. J. Magnet. Magnet. Mater. **505**, 166695 (2020). https://doi.org/10.1016/j.jmmm.2020.166695
13. Szielasko, K., Wolter, B., Tschuncky, R., Youssef, S.: Micromagnetic materials characterization using machine learning. tm - Technisches Messen 87(6), 428–437 (2020) https://doi.org/10.1515/teme-2019-0099
14. Artetxe, I., Arizti, F., Martinez-de-Guerenu, A.: A New Technique to Obtain an Equivalent Indirect Hysteresis Loop From the Distortion of the Voltage Measured in the Excitation Coil. IEEE Trans. Instrum. Meas. **70**, 1–12 (2021). https://doi.org/10.1109/TIM.2020.3022444
15. Artetxe, I., Arizti, F., Martinez-de-Guerenu, A.: Improvement in the Equivalent Indirect Hysteresis Cycles Obtained From the Distortion of the Voltage Measured in the Excitation Coil. IEEE Trans. Instrum. Meas. **70**, 1–11 (2021). https://doi.org/10.1109/TIM.2021.3101327
16. Artetxe, I., Arizti, F., Martínez-de-Guerenu, A.: Analysis of the voltage drop across the excitation coil for magnetic characterization of skin passed steel samples. Measurement **174**, 109000 (2021). https://doi.org/10.1016/j.measurement.2021.109000
17. White, S., Krause, T., Clapham, L.: Control of flux in magnetic circuits for Barkhausen noise measurements. Meas. Sci. Technol. **18**(11), 3501–3510 (2007). https://doi.org/10.1088/0957-0233/18/11/034
18. Stupakov, O.: Investigation of applicability of extrapolation method for sample field determination in single-yoke measuring setup. J. Magnet. Magnet. Mater. **307**(2), 279–287 (2006). https://doi.org/10.1016/j.jmmm.2006.04.015
19. Vértesy, G., Mészáros, I., Tomáš, I.: Nondestructive indication of plastic deformation of cold-rolled stainless steel by magnetic minor hysteresis loops measurement. J. Magnet. Magnet. Mater. **285**(3), 335–342 (2005). https://doi.org/10.1016/j.jmmm.2004.08.006
20. Altpeter, I., Dobmann, G., Kröning, M., Rabung, M., Szielasko, S.: Micro-magnetic evaluation of micro residual stresses of the IInd and IIIrd order. NDT & E Int. **42**(4), 283–290 (2009). https://doi.org/10.1016/j.ndteint.2008.11.007
21. Stupakov, O., Tomáš, I., Kadlecová, J.: Optimization of single-yoke magnetic testing by surface fields measurement. J. Phys. Appl. Phys. **39**(2), 248–254 (2006). https://doi.org/10.1088/0022-3727/39/2/003
22. Moorthy, V.: Distortion analysis of magnetic excitation - a novel method for non-destructive evaluation of depth of surface-hardening in ferritic steels. Philos. Mag. Lett. **94**(9), 564–572 (2014). https://doi.org/10.1080/09500839.2014.944601
23. Moorthy, V.: Distortion analysis of magnetic excitation-a novel approach for the non-destructive microstructural evaluation of ferromagnetic steel. J. Phys. Appl. Phys. **47**(20), 202001 (2014). https://doi.org/10.1088/0022-3727/47/20/202001
24. Moorthy, V.: Distortion analysis of magnetic excitation - Inherent reflection of properties of ferromagnetic materials. J. Magnet. Magnet. Mater. **382**, 58–62 (2015). https://doi.org/10.1016/j.jmmm.2015.01.051
25. Moorthy, V.: Distortion Analysis of Magnetic Excitation (DAME) – A Novel NDE Method for Evaluation of Properties of Ferro-

magnetic Materials. 19th World Conference on Non-Destructive Testing (2016)
26. Kneller, E., Seeger, A., Kronmüller, H.: Ferromagnetismus. Springer Berlin Heidelberg, Berlin, Heidelberg (1962). https://doi.org/10.1007/978-3-642-86695-1
27. Rayleigh: XXV. Notes on electricity and magnetism .—III. On the behaviour of iron and steel under the operation of feeble magnetic forces. Lond. Edinb. Dubl. Phil. Mag. J. Sci. **23**(142), 225–245 (1887) https://doi.org/10.1080/14786448708628000
28. Kachniarz, M., Szewczyk, R.: Study on the Rayleigh Hysteresis Model and its Applicability in Modeling Magnetic Hysteresis Phenomenon in Ferromagnetic Materials. Acta Phys. Pol. A **131**(5), 1244–1250 (2017) https://doi.org/10.12693/APhysPolA.131.1244
29. Feldtkeller, R.: Theorie der Spulen und Überträger, 5th edn. Monographien der elektrischen Nachrichtentechnik, vol. 13. Hirzel, Stuttgart (1971)
30. Youssef, S., Zimmer, C., Kopp, M., Szielasko, K., Farajian, M., Eichheimer, C., Luke, M.: Trennung von Spannungs- und Gefügeeinflüssen in der zerstörungsfreien mikromagnetischen Werkstoffcharakterisierung zur Bewertung der Anlagensicherheit, StressLess Phase II : Abschlussbericht : Berichtsdatum: 01.05.2018 bis 30.04.2020. Trennung von Spannungs- und Gefügeeinflüssen in der zerstörungsfreien mikromagnetischen Werkstoffcharakterisierung zur Bewertung der Anlagensicherheit, StressLess Phase II (2020) https://doi.org/10.2314/KXP:1757680403